Biosensors and Bioelectronics 42 (2013) 532–538

Contents lists available at SciVerse ScienceDirect

Biosensors and Bioelectronics

journal homepage: www.elsevier.com/locate/bios

An integrated sensing system for detection of cholesterol based on TiO_2–graphene–Pt–Pd hybrid nanocomposites

Shurui Cao [a,b], Lei Zhang [b], Yaqin Chai [a], Ruo Yuan [a,*]

[a] Education Ministry Key Laboratory on Luminescence and Real-Time Analysis, College of Chemistry and Chemical Engineering, Southwest University, Chongqing 400715, China

[b] Chongqing Entry Exit Inspection and Quarantine Bureau, Chongqing 400020, China

ARTICLE INFO

Article history:
Received 26 July 2012
Received in revised form
8 October 2012
Accepted 15 October 2012
Available online 26 October 2012

Keywords:
Cholesterol
Graphene sheets (GS)
TiO_2
Pt–Pd
Au nanoparticles (AuNPS)
Cholesterol oxidase (ChOx)

ABSTRACT

In this article, we used the TiO_2–graphene–Pt–Pd hybrid nanocomposites (TGPHs) as an enhanced element of the integrated sensing platform for increasing the surface area as well as improving the electronic transmission rate. Subsequently, Au nanoparticles (AuNPS) and cholesterol oxidase (ChOx) were successively self-assembled to TGPHs with high load amount and superior biological activity. The morphology of TGPHs and stepwise fabrication processes were characterized with cyclic voltammetry (CV), atomic force microscopy (AFM), X-ray photoelectron spectroscopy (XPS) and scanning electron microscopy (SEM). Based on the efficiently catalytic ability of TGPHs and AuNPS, the fabricated biosensor exhibited wide linear ranges of responses to cholesterol in the concentration ranges of $5.0\times10^{-8}-5.9\times10^{-4}$ M, the limit of detection was 0.017 μM (S/N=3). The response time was less than 7 s and the Michaelis–Menten constant (K_m^{app}))was found as 0.21 mM. The fabricated biosensor was further tested using real food samples egg, meat, margarine and fish oil, showing that the biosensor has the potential to be used as a facile cholesterol detection tool in food and supplement quality control.

1. Introduction

Cholesterol is a soft, waxy substance. It is made by the liver as well as being part of a healthy dietary intake of fats. Cholesterol and its fatty acids are important components of nerve and brain cells and are also used in making hormones, vitamin D, and producing energy (Cheng et al., 2011; Chen, 2011). The balanced quantity of cholesterol in human body provides durability and integrity to the cell architecture. Its decreased levels may result in maladsorption, anemia, hyperthyroidism and elevated levels may lead to myxedema, atherosclerosis, diabetes milletus, nephrosis and jaundice (Ding et al., 2011; Malik and Pundir, 2002). Cholesterol exists in the majority of food. For example, the animal's brain content the highest cholesterol, second is in egg yolk and animal visceral. Fish, milk, ice cream and meat also content some cholesterol. However, beans almost have no cholesterol (Basu et al., 2007). In order to guide our body for good health, we need to deploy food reasonably and have a complete profile of the level of cholesterol in our food. The development of efficient rapid analytical methods for estimation cholesterol in food is of great importance. Owing to the advantages of simplicity, rapidness, good selectivity, low volume and cost effectiveness, many electrochemical cholesterol biosensors have been developed which are based on Cytochrome P450scc (Shumyantseva et al., 2004), cholesterol oxidase (ChOx) (Situmorang et al., 1999; Brahim et al., 2001; Tan et al., 2005; Vidal et al., 2004; Ram et al., 2001), ChOx and cholesterol esterase (ChEt) (Li et al., 2005; Singh et al., 2004).

ChOx is most commonly used as the biosensing element. It catalyzes the oxidation of cholesterol to cholest-4-en-3-one and H_2O_2 in the presence of oxygen and the redox property of H_2O_2 can be used to constitute a protocol for its electrochemical determination, which can be detected amperometrically (Ahn and Sampson, 2004; Baby et al., 2011; Huang et al., 2011). Great efforts have been made to enhance the electron transfer in biosensor design by immobilizing ChOx in suitable immobilization matrix. Graphene sheets (GS) as a two-dimensional macromolecular sheet of carbon atoms has high surface area, fast electron transportation, excellent mechanical stiffness, good biocompatibility and can be the ideal conductive additive for hybrid nanostructured electrodes (Berger et al., 2006; Stankovich et al., 2006; Geim, 2009; Ramanathan et al., 2008). Literatures show that decorating inorganic materials with modified grapheme could enhance their electrocatalytic (Li et al., 2009; Seger and Kamat, 2009), electronic (Sun et al., 2010; Wang et al., 2009) and photocatalytic (Zhang et al., 2010; Wu et al., 2010) properties. TiO_2 has been extensively studied to demonstrate the effectiveness of nanostructure and conductive coating (Kavan et al., 1996; Armstrong et al., 2004; Moskon et al., 2006), which have been widely used to immobilize enzymes or proteins on electrode

* Corresponding author. Tel.: +86 23 68252277; fax: +86 23 68254000.
E-mail address: yuanruo@swu.edu.cn (R. Yuan).

0956-5663/$ - see front matter © 2012 Elsevier B.V. All rights reserved.
http://dx.doi.org/10.1016/j.bios.2012.10.048

surface for either fabricating electrochemical biosensors or mechanistic study of the proteins, owing to its abundance, effectiveness, cheapness and chemical stability (Wang et al., 2010; Mun et al., 2010; Ji et al., 2009; Zhuo et al., 2011). Thus, nanostructured TiO_2–graphene hybrid materials were prepared and introduced for binding nano-Au and ChOx in this work. Because of the good biocompatibility and large surface area of nano-Au/TiO_2–graphene, the large load amount of ChOx were obtained on the nano-Au/TiO_2–graphene surface with superior biological activity, which resulted in the improvement of the intensity of the signal and ultrasensitive detection.

Bimetallic alloys have been widely studied and applied in sensor and electrochemistry fields. Owing to the interaction between two components in bimetallic alloys, they generally exhibit many favorable properties that surpass those of their monometallic analogs, which include high catalytic activity, catalytic selectivity, and better resistance to deactivation (Maris et al., 2007; Safavi and Farjami, 2011). Many researchers also have reported that Pt–Au and Pt–Pd alloy were applied in electrochemical sensors displayed high electrocatalytic activity, high sensitivity, fast response time, wide linear range in response to glucose (Habrioux et al., 2007; Bai et al., 2008; Wang et al., 2008) and cholesterol (Safavi and Farjami, 2011).

In this article, we developed a multi-step chemical approach to synthesize nanostructured TiO_2–graphene–Pt–Pd hybrid materials (TGPHs) through self-assembly and electrodeposition techniques. Such TGPHs have several advantages for the design of ChOx-based electrochemical biosensor. (1) Nanostructured TiO_2-graphene hybrid materials (TGHs) have good surface chemical property, where Pt–Pd alloy can exhibit unique catalytic properties. (2) Pt–Pd alloy have high catalytic activity, electronic conductivity, which can accelerate response time and widen linear range. (3) TGPHs have good biocompatibility and can enlarge the electrode area, which is important for enhancing the detection performance. In view of the advantageous features of TGPHs, a sensitive ChOx electrochemical biosensor was constructed using cholesterol as the model analyte. The details of the attractive response performances of the ChOx biosensor and potential merits for cholesterol detection are substantiated as follows.

2. Experimental

2.1. Reagents and materials

Graphene sheets were obtained in Pioneer Nanotechnology Co. (Nanjing, China). Cholesterol oxidase (ChOx, EC 1.1.3.6, ≥ 50 units/mg, from Brevibacterium sp.), cholesterol ($C_{27}H_{46}O$, Mr: 386.67, $\geq 99\%$ purity, from lanolin), Triton X-100 ($C_{34}H_{62}O_{11}$, MW: 646.85), $HAuCl_4$, H_2PtCl_6, $PdCl_2$, Sodium dodecyl sulfate (SDS), sodium citrate, H_2O_2, $TiCl_3$, poly (diallyldimethylammonium chloride) (PDDA, 20% aqueous solution) were obtained from Sigma Chemical Co. (St. Louis, MO, USA). Distilled water was used throughout this study. Phosphate buffered solutions (PBS) (pH 7.0) were prepared using 0.1 M Na_2HPO_4, 0.1 M KH_2PO_4, 0.1 M KCl and kept at 4 °C before use. The stock solution was prepared by dissolving cholesterol in the mixture of 2-propanol and Triton X-100, and then diluted it only with Triton X-100 solution for preparing standard solutions. According to the literature (Enustun and Turkevich, 1963), AuNPs were produced by reducing $HAuCl_4$ with sodium citrate at 100 °C for 0.5 h. The diameter of AuNPs was about 16 nm, which was estimated from transmission electron microscopy (the graph not shown). All other chemicals were of analytical grade and used as received without further purification.

2.2. Apparatus

The cyclic voltammetric (CV) experiments were carried out on a CHI 600D electrochemistry workstation (Shanghai CH InstrumentsInstruments, China), connected to a personal computer. All experiments were performed with a conventional three-electrode system. The modified glassy carbon electrode (GCE) as working electrode, a platinum wire as counter electrode and a saturated calomel electrode (SCE) or Ag/AgCl (sat. KCl) as reference electrode. The assembling interface was tracked by scanning electron microscopy (SEM, S-4800, Hitachi, Japan) and atomic force microscopy (AFM, Veeco, Woodbury, NY, USA). X-ray photoelectron spectroscopy (XPS) measurements were performed with a VG Scientific ESCALAB 250 spectrometer, using Al Ka X-ray (1486.6 eV) as the light source. The pH measurements were made with a pH meter (MP 230, Mettler-Toledo, Switzerland).

2.3. Synthesis of nanostructured TiO_2–graphene hybrid materials

The synthesis of nanostructured TiO_2–graphene hybrid materials (TGHs) were performed according to the literature (Wang et al., 2009). Firstly, 60 mg of GS and 3 mL of SDS aqueous solution (0.5 M) were mixed together. The mixture was diluted to 15 mL and sonicated for 15 min. Then, a portion of 25 mL $TiCl_3$ (0.12 M) aqueous solution was added into as-prepared SDS-GS dispersions while stirring. Finally, 2.5 mL of H_2O_2 (1 wt%) was added dropwise followed by distilled water under vigorous stirring until reaching a total volume of 80 mL. The resulting mixtures were further stirred in a sealed polypropylene flask at 90 °C for 16 h. The precipitates were separated by centrifuge followed by washing with deionized water and ethanol. The centrifuging and washing processes were repeated three times. The product was then dried in a vacuum oven at 70 °C overnight and subsequently calcined in static air at 400 °C for 2 h. The TGHs were dispersed in PDDA solution (1 mg/mL) for future use.

2.4. Fabrication of the proposed biosensor

A glassy carbon electrode (GCE) with 4 mm diameter was firstly polished with 0.3 and 0.05 μm alumina to obtain mirror-like surface, respectively. To remove the physically adsorbed substance, it was rinsed with deionized water and ethanol in ultrasonic bath and dried at room temperature.

Firstly, 1 mg TGHs were dissolved in 1 mL 1% PDDA solution by ultrasonic dispersion, 10 μL of the resulting suspension were coated onto a pretreated GCE surface and dried in the air. Secondly, the electrochemical deposition of Pt–Pd was performed on TGHs modified GCE to form TGPHs in aqueous solution containing 0.5 mM H_2PtCl_6 and 0.5 mM $PdCl_2$. The deposition time was 200 s and the potential was −0.2 V. Then, 10 μL of TGHs were dropped onto the modified TGPHs/GCE surface again and dried in the air. Next, nano-Au monolayer was obtained by immersing the modified GCE into the prepared AuNPs colloid solution for 5 h. Subsequently, 6 μL ChOx (1 mg/mL in 0.1 M PBS, pH 7.0) solutions were dropped on the surface of the electrode to construct a cholesterol biosensor (noted as ChOx/AuNPs/TGHs/TGPHs/GCE). Ultimately, the obtained biosensor was stored at 4 °C when not in use. Fig. 1 showed the schematic diagram of the fabrication of the cholesterol biosensor.

3. Results and discussion

3.1. Characteristics of the TGHs and TGPHs by XPS and SEM

XPS analysis provides effective information on the chemical composition of the as-prepared TGHs. As shown in Fig. 2A, the

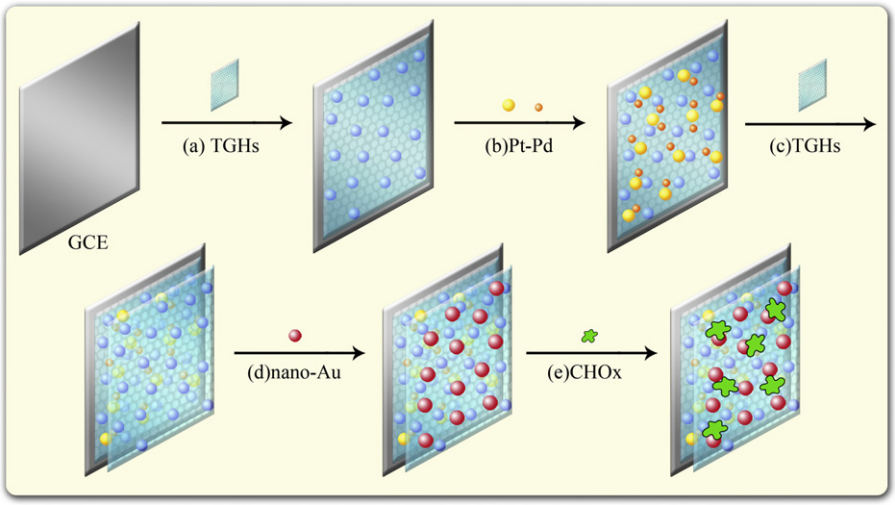

Fig. 1. Schematic diagram of the fabrication of the cholesterol biosensor.

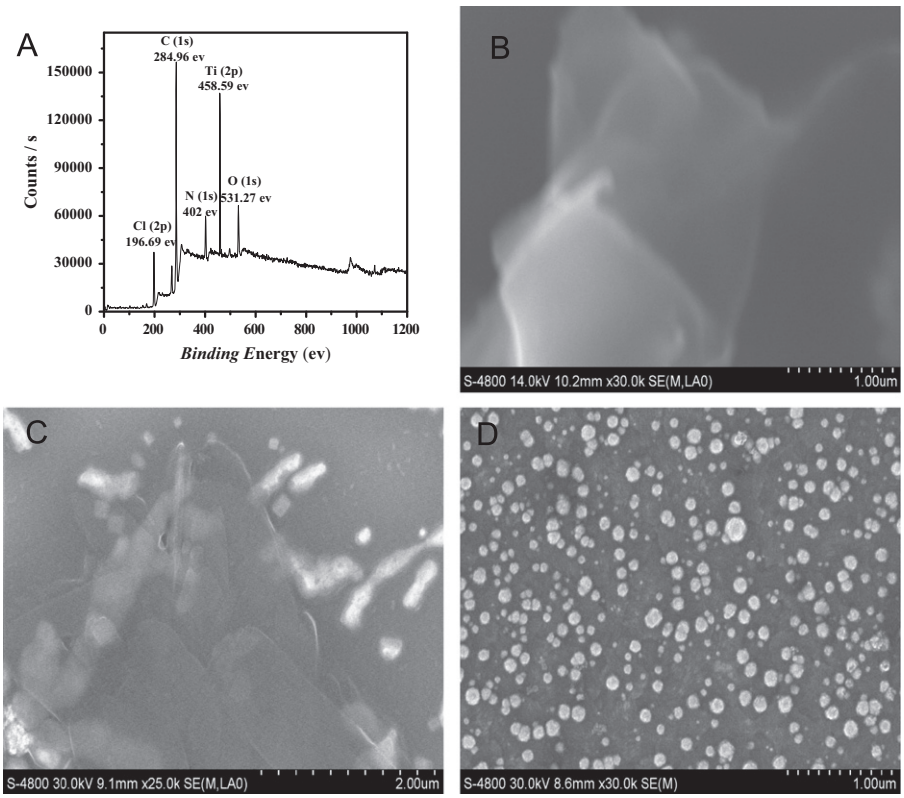

Fig. 2. XPS spectra of TGHs (A), SEM images of GS (B), TGHs (C), and TGPHs (D).

C, Ti, O, N, Cl peaks appeared in the XPS survey spectrum for TGHs, it indicated the TGHs was composed of C, Ti, O, N and Cl elements. It also revealed the reduction of $TiCl_3$ on the surface of GS and the TGHs was synthesized successfully. In order to further confirm the microstructure and morphology of as-prepared nanomaterials, scanning electron microscopy (SEM) were used to investigate. Fig. 2B displays a wrinkled paper-like structure with irregular size, which is the standard morphology of GS. In Fig. 2C, TiO_2 nanoparticles grow in the GS network in irregularly quadrateshaped and appear as bright dots, which indicated that the TGHs was synthesized successfully. After the formation of TGPHs nanomaterials, Pt–Pd alloy NPs were well dispersed in the TGHs network, forming an interpenetrating network for favorable conduction pathways of electron transfer (Fig. 2D).

3.2. Characteristics of proposed biosensor

AFM is used to investigate the interfacial changes of the electrode surface during the fabrication process. Typical AFM images of Au substrate modified with different materials were shown in Fig. 3. As can be seen from Fig. 3A, the image of TGHs film presented a wrinkled homogeneous surface and its root mean square (RMS) roughness was 50.384 nm. When Pt–Pd alloy NPs was electrochemically deposited on TGHs to form TGPHs, the height profile obviously became rougher to a greater extent

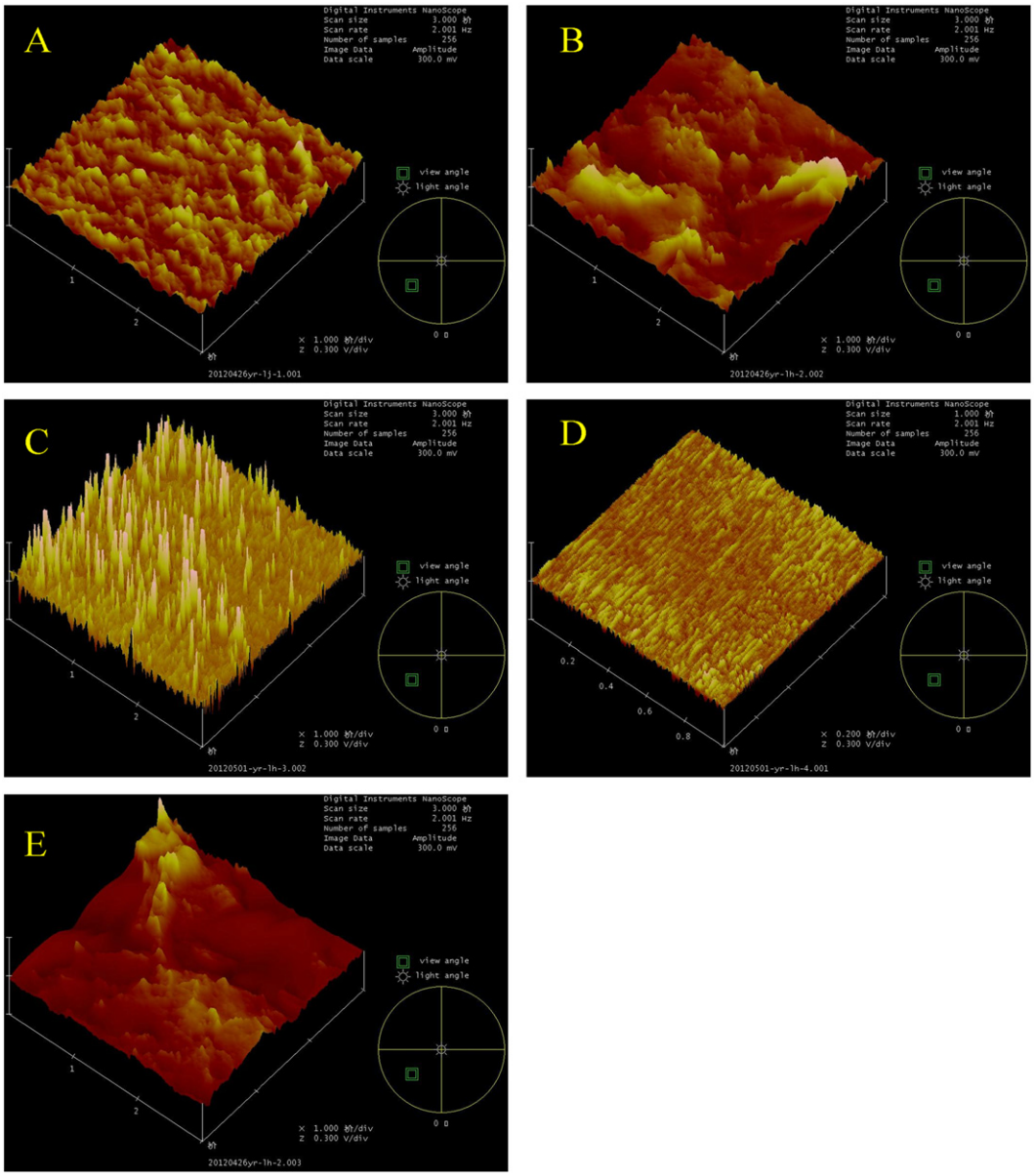

Fig. 3. AFM images of differently modified Au substrates, (A) TGHs/Au, (B) TGPHs/Au, (C) TGHs/TGPHs/Au, (D) AuNPs/TGHs/TGPHs/Au and (E) ChOx/AuNPs/TGHs/TGPHs/Au.

(Fig. 3B) with more electroactive sites and larger surface area (RMS was 75.672 nm). Then, TGPHs was further modified with TGHs (Fig. 3C), the surface morphology was even wrinkled and curled into mountain peak-like structures, further increasing roughness and surface area (RMS was 126.572 nm). After AuNPs were assembled on the TGHs/TGPHs films, the AFM image of AuNPs/TGHs/TGPHs films (Fig. 3D) exhibited a smooth effect as compared to that of TGHs/TGPHs films (RMS was 117.433 nm), AuNPs occupy almost all of the surface of TGHs/TGPHs with fairly even, ordered, and close-packed distribution and therefore provided a good membrane-forming ability with larger surface coverage on substrate. As ChOx was immobilized, a fairly smooth film formed with clear island-like structures and small cracks (Fig. 3E), providing a good platform for biosensing (RMS was 130.260 nm).

In addition, the cyclic voltammetric (CV) behavior of the step by step surface modification of the GCE in 5 mM potassium ferricyanide solution (pH 7.4) containing 0.1 M KCl from −0.2 to 0.6 V at a scan rate of 50 mV/s is shown in Fig. S1. As can be seen, the CV wave of bare GCE showed a well defined redox wave, corresponding to the reversible redox reaction of ferricyanide ions (curve a). After the TGHs composite was modified on the surface of GCE, the peak current of the modified electrode decreased (curve b), indicating that the TGHs composite had been immobilized successfully. When Pt–Pd alloy NPs was electrochemically deposited on TGHs to form TGPHs, the peak current increased markedly (curve c) for the reason that Pt–Pd alloy NPs could facilitate electron transfer between biomolecules and electrode surface. Then, TGPHs was further modified with TGHs, a decreased peak current was acquired (curve d), this may be the reject effect between potassium ferricyanide solution and PDDA. After AuNPs were adsorbed in the TGHs/TGPHs films (curve e), an increased peak current was obtained owing to AuNPs that may act as a bridge of electron transfer and promote the electron transfer. As ChOx was successively loaded onto the electrode surface, curve f in Fig. S1 shows that the voltammetric response decreases as the formation of a hydrophobic protein layer which insulates the conductive support and the interfacial electron transfer.

3.3. The comparison of different signal amplification strategies

In order to evaluate the effect of TGHs, TGPHs, TGHs/TGPHs and AuNPs/TGHs/TGPHs films for the signal amplification, four kinds of ChOx biosensors were prepared and the results are shown in Fig. 4. The different ChOx biosensors are: (a) ChOx/TGHs/GCE, (b) ChOx/TGPHs/GCE, (c) ChOx/TGHs/TGPHs/GCE and (d) ChOx/AuNPs/TGHs/TGPHs/GCE. To control the reaction condition, the amperometric responses of the four kinds of ChOx biosensors were recorded at a potential of −0.35 V (versus SCE) in 0.1 M PBS (pH 7.0) after successive additions of 0.5 mM cholesterol, respectively. It can be found that the ChOx/AuNPs/TGHs/TGPHs/GCE biosensor offered highest response currents than that obtained for the other three biosensors. This visible enhancement can be attributed to the large surface area of the AuNPs/TGHs/TGPHs, which can immobilize more ChOx and keep the good biological activity of ChOx.

3.4. Optimization of main experimental conditions

It is important to control the optimal experimental conditions to obtain the excellent performance of the biosensor for cholesterol detection. Several key parameters, such as the deposition time of Pt–Pd alloy NPs, pH of the detection solution and potential of detection were optimized by CVs. To further study the catalytic property of ChOx/AuNPs/TGHs/TGPHs/GCE, the influence of the deposition time of Pt–Pd alloy NPs was investigated on the response current of cholesterol (not shown). With the increase in deposition time from 50 to 300 s, the response current enhanced but further increase in deposition time caused the current to slightly decrease, indicating that the electrochemical active surface area has been decreased. Therefore, the optimum deposition time was 200 s.

As the pH of the detection solution might influence the activity of ChOx, the pH dependence of the voltammetric response was investigated over the pH values from 5.5 to 8.5 in the detection solution containing 0.5 mM cholesterol (Fig. S2(A)). It was found that the biosensor displayed an optimum sensitivity of the response at pH 7.0, indicating that the biosensor is more active at this pH and the immobilized ChOx retain its natural structure and do not denature. Thus, the optimal pH of 7.0 was chosen in the further study.

The dependence of the ChOx biosensor response on the applied potential was evaluated over the potential range from −0.55 to 0.0 V for cholesterol in 0.1 M PBS (pH 7.0) (Fig. S2(B)). The optimal applied potential can be observed at −0.35 V vs. SCE. Consequently, an operational potential value of −0.35 V was chosen for subsequent amperometric measurements for cholesterol.

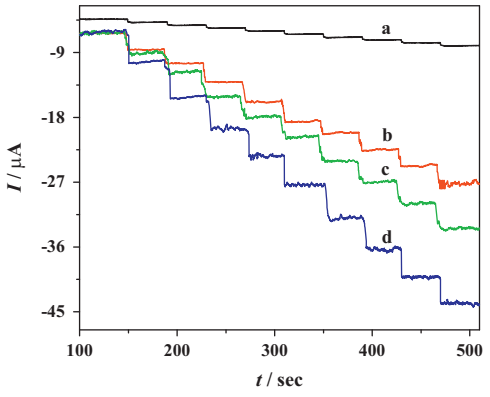

Fig. 4. Response current–time curves of variously modified electrodes, (a) ChOx/TGHs/GCE, (b) ChOx/TGPHs/GCE, (c) ChOx/TGHs/TGPHs/GCE, (d) ChOx/AuNPs/TGHs/TGPHs/GCE to the successive addition of 0.5 mM cholesterol in PBS (0.1 M, pH 7.0).

3.5. The quantificational detection of cholesterol

The analytical performance of the prepared ChOx biosensor was explored by quantifying the standard cholesterol solution with different concentrations according to the described conditions. Fig. 5(A) displays the typical amperometric response of the biosensor based on integrated sensing system for successive injection of cholesterol to stirring 5 mL 0.1 M PBS at pH 7.0. As expected, the amperometric response increased with the concentration of cholesterol. The standard calibration curve for cholesterol detection is shown in Fig. 5(B). It can be found the linear range covered from 5.0×10^{-8} to 5.9×10^{-4} M with a correlation coefficient of 0.9994. The detection limit corresponding to three times the standard deviation of the blank solution was estimated as 0.017 μM. Furthermore, the analytical performances of the proposed biosensor were compared with those cholesterol sensors, as summarized in Table 1. It could be found that the proposed biosensor exhibited satisfactory detection limit and linear range. The reasons might be that the relatively large amounts of ChOx were immobilized onto AuNPs/TGHs/TGPHs multilayers, which could enhance the access chance of the ChOx and cholesterol.

The apparent Michaelis–Menten constant (K_m^{app}), which gives an indication of the enzyme–substrate kinetics, can be estimated from the Lineweaver–Burk equation (Kamin and Wilson, 1980). The K_m^{app} of the prepared ChOx biosensor was calculated to be

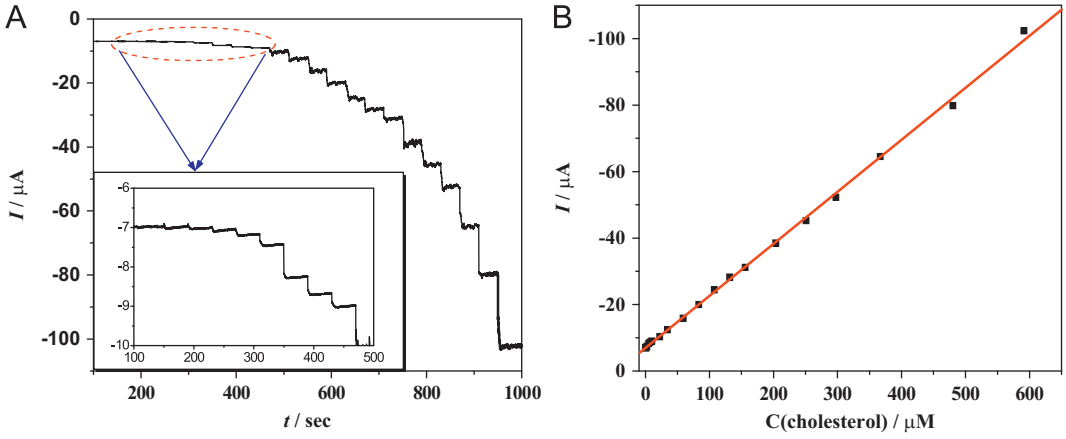

Fig. 5. Amperometric responses for increasing cholesterol concentrations at the biosensor in 5 mL 0.1 M PBS at pH 7.0 (A) and the calibration curve (B).

Table1
Comparison of the responses of some cholesterol biosensors constructed based on different modified electrode materials.

Electrode	K_m^{app} (mM)	Linear ranage (M)	Detection limit (M)	Reference
(MWNTs)–Au/PPD–ChOx	7.17	$5.0\times10^{-4}-6.0\times10^{-3}$	2.0×10^{-4}	Guo et al. (2004)
Chit-Hb/Chit- ChOx	–	$1.0\times10^{-5}-6.0\times10^{-4}$	9.5×10^{-6}	Zhao et al. (2008)
PTMSPA-HRP/ChOx-ME	–	$1.0\times10^{-3}-2.5\times10^{-2}$	5.0×10^{-4}	Manesh et al. (2010)
Chit-LDHs/HRP/ChOx	–	$4.0\times10^{-8}-6.0\times10^{-4}$	$4.0-10^{-8}$	Ding et al. (2011)
IL-Ch-AuPt/ChOx	0.24	$5.0\times10^{-5}-6.2\times10^{-3}$, $6.2\times10^{-3}-11.2\times10^{-3}$,	1.0×10^{-5}	Safavi and Farjami (2011)
Ti/NPAu/ChOx–HRP–ChE	0.64	$9.7\times10^{-4}-7.8\times10^{-3}$	–	Ahmadalinezhad, and Chen (2011)
TGPHs/TGHs/AuNPsChOx	0.21	$5.0\times10^{-8}-6.0\times10^{-4}$	1.7×10^{-8}	This work

0.21 mM, which is much lower than the cholesterol biosensors reported in literature (Table 1). The small K_m^{app} value indicates that the immobilized enzymes possess high enzymatic activity and that the fabricated biosensor exhibits a high affinity for cholesterol.

3.6. The selectivity, reproducibility and stability of the biosensor

The selectivity of biosensor plays a crucial role in their application to the sample analysis. To affirm the selectivity of the proposed ChOx biosensor, possible interference of ascorbic acid (AA), uric acid (UA), dopamine (DA) and glucose on the current response of the cholesterol sensors was shown in Fig. S3. The amperometric response to successive additions of 1 mM AA, 1 mM UA, 1 mM DA and 5 mM glucose were insignificant, but when 0.5 mM cholesterol were successively added, the response to cholesterol was very strong. It suggests that the selectivity of the biosensor was acceptable. The negligible interference on the current response of enzyme catalysis may be due mainly to the negative working potential.

The reproducibility of the analytical responses obtained from different electrodes constructed by the same procedure was analyzed. Seven different electrodes were tested independently for these amperometric responses to 0.5 mM cholesterol. The results revealed that the relative standard deviation (RSD) value for all seven electrodes was 4.7%. The stability of the biosensor was also determined by measuring change in the current response at regular interval of 3 days for 4 weeks. When not used, the biosensor was stored at 4 °C. The results indicated that 89.4% of the response current of the cholesterol sensor were retained after four weeks.

3.7. Real sample analysis

The developed ChOx biosensor was further tested using real food samples egg, meat, margarine and fish oil. The real samples were prepared using the same procedure as the cholesterol solution described in Section 2.1. The amount of cholesterol found in egg, meat, margarine and fish oil was 382.12, 88.94, 0.21 and 40.98 mg/100 g, respectively. This is in good agreement with the amount of the cholesterol listed on the product labels which have been tested by high performance liquid chromatography. All these results show that the fabricated cholesterol biosensor offers a great potential of application in cholesterol quality control of food products.

4. Conclusions

In conclusion, a rapid and selective cholesterol biosensor was constructed based on AuNPs/TGHs/TGPHs composite film. The nanocomposite film can provide a favorable microenvironment for ChOx and effectively keep their activities. Due to the low background response and the improved high load amount and activity of the ChOx, the sensitivity of the biosensor for cholesterol was enhanced with a detection limit of 0.017 μM, a value below the commonly reported in recent literatures. Besides, the developed ChOx biosensor showed highly anti-interferences behavior as tested toward common interfering species such as AA, UA, DA and glucose. Furthermore, the developed biosensor was also successfully used to measure cholesterol in real food samples, showing that the biosensor has the potential to be used as a facile cholesterol detection tool in food and supplement quality control.

Acknowledgments

This work was supported by National Natural Science Foundation of China (21075100), the Ministry of Education of China (Project 708073), the Nature Science Foundation of Chongqing City (CSTC-2011BA7003 and CSTC-2009BA1003) and Specialized Research Fund for the Doctoral Program of Higher Education (20100182110015).

Appendix A. Supporting information

Supplementary data associated with this article can be found in the online version at http://dx.doi.org/10.1016/j.bios.2012.10.048.

References

Ahmadalinezhad, A., Chen, A.C., 2011. Biosensors and Bioelectronics 26, 4508–4513.
Ahn, K.W., Sampson, N.S., 2004. Biochemistry 43, 827–836.
Armstrong, A.R., Armstrong, G., Canales, J., Bruce, P.G., 2004. Angewandte Chemie-International Edition 43, 2286–2288.
Baby, T.T., Arockiadoss, T., Rakhi, R.B., Ramaprabhu, S., 2011. Thin Solid Films 519, 5667–5672.
Bai, Y., Sun, Y., Sun, C., 2008. Biosensors and Bioelectronics 24, 579–585.
Basu, A.K., Chattopadhyay, P., Roychoudhuri, U., Chakraborty, R., 2007. Bioelectrochemistry 70, 375–379.
Berger, C., Song, Z.M., Li, X.B., Wu, X.S., Brown, N., Naud, C., Mayo, D., Li, T.B., Hass, J., Marchenkov, A.N., Conrad, E.H., First, P.N., De Heer, W.A., 2006. Science 312, 1191–1196.
Brahim, S., Nariresingh, D., Guiseppi,_, E.A., 2001. Analytica Chimica Acta 448, 27–36.
Chen, A., 2011. Biosensors and Bioelectronics 26, 4508–4513.
Cheng, F., He, J.S., Zhen, C.C., 2011. Sensors and Actuators, B 155, 545–550.
Ding, S.N., Shan, D., Zhang, T., Dou, Y.Z., 2011. Journal of Electroanalytical Chemistry 659, 1–5.
Enustun, B.V., Turkevich, J.J., 1963. Journal of the American Chemical Society 85, 3317–3328.
Geim, A.K., 2009. Science 324, 1530–1534.
Guo, M., Chen, J., Li, J., Nie, L., Yao, S., 2004.
Habrioux, A., Sibert, E., Servat, K., Vogel, W., Kokoh, K.B., Alonso-Vante, N., 2007. Journal of Physical Chemistry B 111, 10329–10333.
Huang, Q.L., An, Y.R., Tang, L.l., Jiang, X.L., Chen, H., Bi, W.J., Wang, Z.C., Zhang, W., 2011. Analytica Chimica Acta 707, 135–141.
Ji, J., Yang, H., Liu, Y., Chen, H., Kong, J.L., Liu, B.H., 2009. Chemical Communications 12, 1508–1510.
Kamin, R.A., Wilson, G.S., 1980. Analytical Chemistry 52, 1198–1205.

Kavan, L., Gratzel, M., Rathousky, J., Zukal, A., 1996. Journal of the Electrochemical Society 143, 394–400.
Li, G., Lia, J.M, Hu, G.Q., Ma, N.Z., Wu, P.J., 2005. Biosensors and bioelectronics 20, 2140–2144.
Li, Y., Tang, L., Li, J., 2009. Electrochemistry Communications 11, 846–849.
Malik, V., Pundir, C.S., 2002. Biotechnology and Applied Biochemistry 35, 191–197.
Manesh, K.M., Santhosh, P., Gopalan, A.L., Lee, K.P., 2010. Electroanalysis 22, 2467–2474.
Maris, E.P., Ketchie, W.C., Murayama, M., Davis, R.J., 2007. Journal of Catalysis 251, 281–294.
Moskon, J., Dominko, R., Gaberscek, M., Cerc-Korosec, R., Jamnik, J., 2006. Journal of the Electrochemical Society 153, A1805–A1811.
Mun, K.S., Alvarez, S.D., Choi, W.Y., Sailor, M.J., 2010. ACS Nano 4, 2070–2076.
Ram, M.K., Bertoncello, P., Ding, H., Paddeu, S., Nicolini, C., 2001. Biosensors and Bioelectronics 16, 849–856.
Ramanathan, T., Abdala, A.A., Stankovich, S., Dikin, D.A., Herrera-Alonso, M., Piner, R.D., Adamson, D.H., Schniepp, H.C., Chen, X., Ruoff, R.S., Nguyen, S.T., Aksay, I.A., Prud'homme, R.K., Brinson, L.C, 2008. Nature Nanotechnology 3, 327–331.
Safavi, A., Farjami, F., 2011. Biosensors and Bioelectronics 26, 2547–2552.
Seger, B., Kamat, P.V., 2009. Journal of Physical Chemistry C 113, 7990–7995.
Shumyantseva, V., Deluca, G., Bulko, T., Carrara, S., Nicolini, C., Usanov, S.A., Archakov, A, 2004. Biosensors and Bioelectronics 19, 971–976.
Singh, S., Chaubey, A., Malhotra, B.D., 2004. Analytica Chimica Acta 502, 229–234.
Situmorang, M., Alexander, P.W., Hibbert, D.B., 1999. Talanta 49, 639–649.
Stankovich, S., Dikin, D.A., Dommett, G.H.B., Kohlhaas, K.M., Zimney, E.J., Stach, E.A., Piner, R.D., Nguyen, S.T., Ruoff, R.S., 2006. Nature 442, 282–286.
Sun, S., Gao, L., Liu, Y., 2010. Applied Physics Letters 96, 083113.
Tan, X., Li, M., Cai, P., Luo, L., Zou, X., 2005. Analytical Biochemistry 337, 111–120.
Vidal, J.C., Espuelas, J., Ruiz, G.E., Castillo, J.R., 2004. Talanta 64, 655–664.
Wang, D.H., Choi, D.W., Li, J., Yang, Z.G., Nie, Z.M., Kou, R., Hu, D.H., Wang, C.M., Saraf, L.V., Zhang, J.G., 2009. ACS Nano 3, 907–914.
Wang, J., Thomas, D.F., Chen, A., 2008. Analytical Chemistry 80, 997–1004.
Wang, Y., Ma, X.L., Wen, Y., Xing, Y.Y., Zhang, Z.R., Yang, H.F., 2010. Biosensors and Bioelectronics 25, 2442–2446.
Wu, J., Shen, X., Jiang, L., Wang, K., Chen, K., 2010. Applied Surface Science 256, 2826–2830.
Zhang, H., Lv, X., Li, Y., Wang, Y., Li, J., 2010. ACS Nano 4, 380–386.
Zhao, C.Z., Wan, L., Jiang, L., Wang, Q., Jiao, K., 2008. Analytical Biochemistry 383, 25–30.
Zhuo, Y., Chai, Y.Q., Yuan, R., Mao, L., Yuan, Y.L., Han, J., 2011. Biosensors and Bioelectronics 26, 3838–3844.